TABLE V
NUMBER OF ANALYZED IMAGES OF CONTROL AND PUNCTURED SAMPLES, GROUPED BY VARIETY AND VINTAGE

		cv. Williams		cv. Abate Fétel	
2022	Control	250	304	403	624
	Punctured	54		221	
2023	Control	353	651	251	352
	Punctured	298		101	

As detailed in [50], we covered tree branches with exclusion cages on fruit set to safeguard the flowers and ripening fruits from uncontrolled biotic and abiotic adversities. These exclusion cages consist of a semirigid black plastic mesh covered by a sleeve made of fabric mesh. Approximately one week prior to harvesting, we placed BMSB specimens inside half of the exclusion cages, while we used the fruits in the remaining exclusion cages as control samples.

The monitoring of fruit damages occurred at eight subsequent acquisition times, from harvesting (T1) until five weeks later (T2–T8). After harvesting, we stored the fruits at 6–8°C for 1–2 days to avoid chilling damages, then we gradually lowered the temperature to 0–4 °C to simulate postharvest refrigeration conditions. Then, we acquired hyperspectral images using a SNAPSCAN SWIR camera (IMEC, One Planet), covering the 1156–1674 nm spectral range. Before imaging each fruit, the acquisition software performed an automatic calibration based on the dark current signal and a high-reflectance standard. For each pear, we acquired four hyperspectral images to consider the whole fruit surface. Following the same procedure, we acquired RGB images of the pear as visual reference both before and after peeling the fruits.

Based on experimental conditions, the collected pear samples can be divided in two groups: samples exposed to BMSB and control samples. However, after peeling the fruits, we observed that not all the exposed samples had been punctured, and that some control fruits presented damages. In addition, some damages found on exposed fruits were not due to BSBM but to other adversities (e.g., moulds). For these reasons, we used the RGB images of unpeeled and peeled samples to visually classify the fruits based on damage type and intensity. This labeling process allowed a better identification of the actual sound and punctured samples, and thus we only considered the images belonging to these two classes for further elaborations. Table V reports the number of images belonging to sound control pears and damaged fruits exposed to BMSB, subdivided by fruit variety and harvest year.

We separately analyzed the hyperspectral images belonging to Abate Fétel and Williams varieties, and before their elaboration, we used SNV and linear detrend as spectra preprocessing methods, respectively. Then, we used an automated procedure based on PCA to mask the fruit area by removing pixels belonging to the background setting, fruit peduncle, and plastic label present in the image scene. Then, we improved the segmentation by applying an erosion morphological operator, using a disk structuring element with a 2-pixel radius.

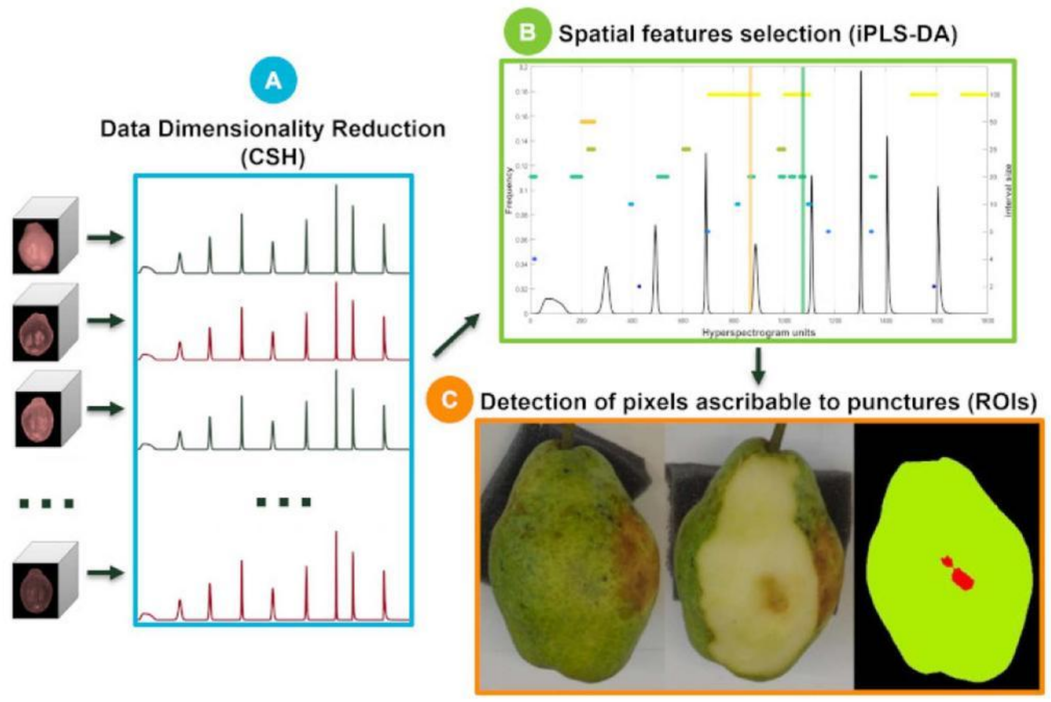

Fig. 8. Schematic representation of the procedure followed for the supervised annotation of BMSB punctures: in (a), data dimensionality reduction of the hyperspectral images using the CSH method, in (b), application of iPLS-DA classification and variable selection algorithm to select the CSH features (i.e., image pixels) related to the punctures, and in (c), image reconstruction of the selected features ascribable to punctures.

B. Supervised Annotation of Punctures

A preliminary exploratory analysis using PCA allowed to distinguish between sound and punctured areas based on slight spectral differences, but at the same time highlighted the difficulty of correctly identifying the regions of interest (ROIs) ascribable to the punctured areas, due to their irregular shapes and the blurred edges between sound and damaged regions. The identification of ROIs belonging to punctured areas is important to extract representative spectra to be used for the development of pixel-level classification models. To overcome this issue, we developed a supervised annotation method to automatically select pixels belonging to punctured areas. The proposed approach is based on data dimensionality reduction of the hyperspectral images using the common space hyperspectrograms (CSH) [51] followed by image-level classification, coupled with feature selection and visualization of the selected features back into the original image domain. More in detail, each image was converted into the corresponding CSH, a 1-D signal obtained by merging in sequence the frequency distribution curves of quantities obtained from a global PCA model[2] (i.e., PC score vectors, Q residuals, and Hotelling T2 values).

Starting from the CSH dataset, we applied the interval PLS-DA (iPLS-DA) algorithm [52] to calculate image-level classification models and select relevant spatial features ascribable to the presence of punctures. Then, we visualized back the selected features of interest into the original image domain, allowing to automatically select ROIs ascribable to punctured areas; this procedure will be referred to as image reconstruction. Fig. 8 shows a schematic representation of such a supervised annotation method.

For both pear varieties, we split the images acquired in 2022 into a training set, used to calculate the common PC space of CSH and calibrate the classification models, and a test set of images used for external validation. We randomly assigned about

[2] A detailed description of the CSH method is in the work of Calvini et al. [51].